



Timing Variations in a Magnetic Pulse Compression Circuit

THESIS

Jeremy S. Oliver, Capt, USAF

AFIT/GE/ENG/12-31

**DEPARTMENT OF THE AIR FORCE
AIR UNIVERSITY**

AIR FORCE INSTITUTE OF TECHNOLOGY

Wright-Patterson Air Force Base, Ohio

DISTRIBUTION STATEMENT A
APPROVED FOR PUBLIC RELEASE; DISTRIBUTION IS UNLIMITED

The views expressed in this thesis are those of the author and do not reflect the official policy or position of the United States Air Force, Department of Defense, or the United States Government. This material is declared a work of the United States Government and is not subject to copyright protection in the United States.

Timing Variations in a Magnetic Pulse Compression Circuit

THESIS

Presented to the Faculty

Department of Electrical and Computer Engineering

Graduate School of Engineering and Management

Air Force Institute of Technology

Air University

Air Education and Training Command

In Partial Fulfillment of the Requirements for the
Degree of Master of Science in Electrical Engineering

Jeremy S. Oliver, BS

Captain, USAF

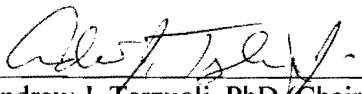
March 2012

DISTRIBUTION STATEMENT A
APPROVED FOR PUBLIC RELEASE; DISTRIBUTION UNLIMITED

Timing Variations in a Magnetic Pulse Compression Circuit

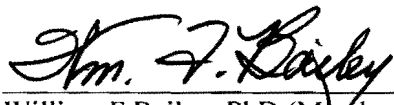
Jeremy S. Oliver, BS
Captain, USAF

Approved:



Andrew J. Terzuoli, PhD (Chairman)

12 Mar 2012
Date



William F Bailey, PhD (Member)

12 Mar '12
Date



Maj Michael C Pochet, PhD (Member)

12 Mar 12
Date

Abstract

The Melville line, also known as a magnetic pulse compression (MPC) circuit, uses saturable core inductors and capacitors to compress the width of a pulse. This substantially increases the peak power of the initially applied pulse. Saturable core inductors, often referred to as magnetic switches, are favorable in pulsed power systems due to their high power capacity, simple design with no moving parts, and ability to generate short pulses.

The saturable inductor exhibits a hysteresis curve behavior. One particular problem with these MPC circuits is timing variances in the pulse rate of the system. These can be caused by several things from poorly regulated power supplies to the saturable inductor not resetting to the initial state after each pulse. This work models the unique characteristics and signatures of the timing variations of magnetic switches and MPC circuits.

The hysteresis curve of the saturable inductor was created by using a nonlinear inductor and a nonlinear resistor in parallel as a substitute for saturable inductors. Measured data provided was used in MATLAB to construct the curves for the nonlinear inductors and nonlinear resistors. Once the circuit was built in MATLAB, simulations were run to determine the effectiveness of the pulse compression as well as the timing delays. The shape of the timing delay plots was caused by the hysteresis curve not resetting to the initial state on the B-H plane after the first pulse is applied and it achieving a steady state at some smaller B-H curve after several pulses.

Acknowledgments

I would like to Dr. Andrew Terzuoli for the patience and guidance during the thesis process. I would like to thank Maj Michael Pochet for his help with circuits and switching technologies and his HPM expertise. I would also like to think Dr. William Bailey for the HPM classes that provided useful information as well as the expertise provided to the problem. I would also like to thank Dr. William Berglund and John Braun for providing me a project and getting me going down the right path. Finally, I would like to thank Stephen Hartzell for the programming help in MATLAB.

Jeremy S. Oliver

Table of Contents

	Page
Abstract.....	iii
Acknowledgments.....	iv
Table of Contents.....	v
List of Figures.....	vii
List of Tables.....	ix
List of Equations.....	x
I. Introduction.....	1
1.1 General Issue.....	1
1.2 Problem Statement.....	2
1.3 Assumptions/Limitations.....	3
1.4 Organization of Thesis.....	3
II. Background Information.....	5
2.1 Chapter Overview.....	5
2.2 Pulsed Power.....	5
2.3 Switches.....	8
2.3.1 Gas Switches.....	9
2.3.2 Semiconductor Switches.....	12
2.3.3 Magnetic Switches.....	13
2.3.4 Switch Summary.....	13
2.4 MPC Circuits.....	14
2.4.1 Hysteresis.....	15
2.4.2 Operation.....	19
2.4.3 Timing Variations.....	22
2.5 Summary.....	25
III. Methodology.....	27
3.1 Chapter Overview.....	27
3.2 Constructing the Model.....	27
3.2.1 Nonlinear Inductor.....	29
3.2.2 Nonlinear Resistor.....	33
3.3 Circuit Parameters.....	35
3.4 Summary.....	37

IV. Analysis and Results.....	38
4.1 Chapter Overview	38
4.2 Simulation Results	38
4.3 Validation of Circuit	41
4.4 Timing Variation Signatures.....	43
4.5 Summary	46
V. Conclusions and Recommendations	47
5.1 Chapter Overview	47
5.2 Conclusions of Research.....	47
5.3 Recommendations for Future Research.....	49
Appendix A – MATLAB Code to Create Nonlinear Inductor Mask.....	50
Appendix B – MATLAB Code to Create Nonlinear Resistor Function	51
Appendix C – MATLAB Code to Calculate Pulse Delay	52
Bibliography	53

List of Figures

	Page
Figure 1 - Illustration of Pulse Compression [1]	2
Figure 2 – Pulse Shape Parameters [2]	6
Figure 3 – Three Electrode Spark Gap [2].....	10
Figure 4 – Magnetic Core B-H Curve [5].....	15
Figure 5 – Two Stage MPC Circuit	19
Figure 6 – Hysteresis Behavior of the Core of a Saturable Inductor [3]	21
Figure 7 – Experimental Output Timing Signature of MPC Circuit used by LLNL for (top) 1 kHz PRF and (bottom) 5 kHz PRF [8].....	25
Figure 8 – Nonlinear Inductor Current versus Flux Curve [9]	28
Figure 9 – Nonlinear Resistor Voltage versus Current Curve [9]	28
Figure 10 – Hysteresis Curve Corresponding to the Nonlinear Inductor and Nonlinear Resistor Provided in Figure 8 and Figure 9 [9]	29
Figure 11 – Nonlinear Inductor Schematic in Simulink	30
Figure 12 - Nonlinear Inductor Mask in Simulink.....	32
Figure 13 - Nonlinear Resistor Schematic in Simulink	34
Figure 14 - Nonlinear Resistor Mask in Simulink	34
Figure 15 – Circuit Layout Used in Simulink for MPC Circuit Simulations	36
Figure 16 - Pulse Shape of the Voltage for a 10 s Simulation for (top) the Input Voltage, (middle) the Voltage across C_2 , and (bottom) the Voltage across the Load.....	39
Figure 17 - Pulse Shape of the Voltage for a single Pulse for (top) the Input Voltage, (middle) the Voltage across C_2 , and (bottom) the Voltage across the Load.....	39

Figure 18 – Pulse for the Current for a 10 s Simulation for (top) the Current through L_1
and (bottom) the Current through L_2 40

Figure 19 – Pulse Shape of the Current for a single Pulse for (top) the Current through L_1
and (bottom) the Current through L_2 40

Figure 20 – MPC Circuit Proposed by Melville [10] 42

Figure 21 – Current Measurements of Melville’s Circuit [10] 42

Figure 22 – Pulse Delay between the Input Pulse and the Output Pulse for a Square Pulse
0.01 s in duration every 1 s 43

Figure 23 - Pulse Delay between the Input Pulse and the Output Pulse for a Square Pulse
0.01 s in duration every 0.1 s 45

Figure 24 - Pulse Delay between the Input Pulse and the Output Pulse for a Square Pulse
0.01 s in duration every 10 s 45

List of Tables

	Page
Table 1 - Comparison of Switch Characteristics [2].....	14

List of Equations

	Page
Equation 1	7
Equation 2	7
Equation 3	18
Equation 4	18
Equation 5	18
Equation 6	18
Equation 7	18
Equation 8	18
Equation 9	19
Equation 10	19
Equation 11	21
Equation 12	21
Equation 13	22
Equation 14	22
Equation 15	22
Equation 16	30
Equation 17	30
Equation 18	33
Equation 19	33

Timing Variations in a Magnetic Pulse Compression Circuit

I. Introduction

1.1 General Issue

High power microwave (HPM) systems have the same basic components as standard microwave ovens. However, an HPM system operates at a much greater power level than a microwave oven. A typical microwave oven generates less than 1,500 watts of power, while an HPM system can generate millions of watts of power. HPM weapons can degrade, deny, and destroy electronics. HPM weapons couple power from the RF and microwave bands into electrical pulses in circuits. Induced high voltages and currents overwhelm normal circuit operation or destroy circuits. Unlike electronic warfare these pulses are not tailored to a specific coupling mechanism or effect. Their generic nature makes protection from HPM much more difficult to accomplish.

HPM systems are comprised of six different modules. There is the prime power and conditioning, microwave source, coupling and transport, antenna, propagation medium, and the receiver or target [1]. This thesis will focus on the prime power and conditioning module of the HPM system. The microwave sources require high-power short-pulse inputs to function properly; due to this constraint, a pulse forming stage is often necessary to compress and properly condition the driving input from the prime power supply.

The pulse compression takes the energy from a low-power long-pulse and increases its voltage or current while shortening the pulse duration. This can be seen in Figure 1. The pulse coming into the pulse compressor can be seen as pulse P_0 . This pulse is then compressed by the first stage of the compressor and can be seen as pulse P_1 . From Figure 1 you can clearly see that the peak power in pulse P_1 is greater than the peak power in pulse P_0 while the duration of pulse P_1 is less than duration of pulse P_0 which is the function of the first stage of the pulse compressor. This continues with pulse P_2 being compressed from pulse P_1 in the same manner by the second stage of the pulse compressor.

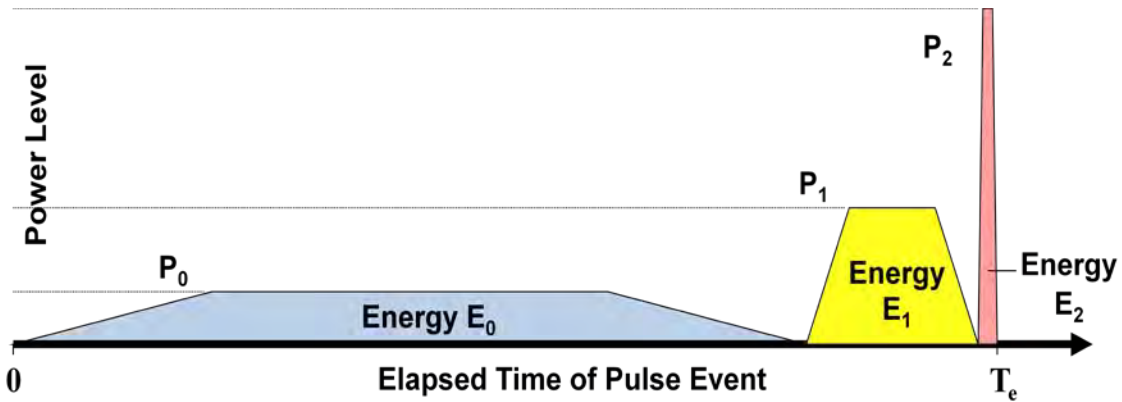


Figure 1 - Illustration of Pulse Compression [1]

1.2 Problem Statement

Magnetic switches and magnetic pulse compression (MPC) circuits are being used more frequently in HPM devices to accomplish pulse compression. The objective of this thesis is to model the unique characteristics and signatures of magnetic switches and MPC

circuits. The particular parameter that will be measured is the time delay of a MPC circuit.

1.3 Assumptions/Limitations

This thesis will evaluate the signature of the MPC circuit only. It will not take into account any fluctuations in the power supply for the pulse compressor. There is no perfect power supply; the output can change depending on temperature or the load seen. Also there is no evaluation of how different loads will affect the signature of the MPC circuit. In addition different temperatures are not taken into account. The temperatures would not only affect the function of the power supply but also the properties of the magnetic materials in the magnetic switches.

1.4 Organization of Thesis

The background information chapter will discuss the theory behind pulse compression, switch technologies, the function of magnetic switches and MPC circuit. The chapter will begin with a discussion on the theory behind pulse compression. The chapter will then discuss different switch technologies used in pulse compression systems and positive properties of the magnetic switch. Next the chapter will provide a detailed summary of how MPC circuits work. This will provide the theoretical basis needed for the rest of the thesis.

The methodology chapter will document how the model in the simulation was created. The chapter will discuss the theory behind using a nonlinear inductor and nonlinear resistor in parallel to model the saturable inductor. Then it will discuss the building of the model in MATLAB Simulink. Finally will be a discussion on the exact parameters of the circuit used in the simulation.

The analysis and results chapter will display the voltage and current pulses produced by the simulation. The figures of the voltage and current will show both the input and the output shape to show the pulse compression. Next will be verification of the simulation data to show that the results can be trusted. This chapter will also include the plots of the timing delays for the simulations to establish a signature for the MPC circuit as well as a discussion on what produced the results.

The conclusions and recommendations chapter will wrap up the discussion on the MPC circuit with a summary of the information presented and the findings of the simulations. Also discussed are any future paths for follow-on work.

II. Background Information

2.1 Chapter Overview

The discussion will begin with a description of pulsed power. After that there will be a discussion on different types of switches that are common in pulse power systems and why the magnetic switch is being considered. Then there is a more detailed description of MPC circuits beginning with a brief description of hysteresis curves, then describing the operation in detail, and finally moving to a discussion of the timing variations in the MPC circuit.

2.2 Pulsed Power

The discussion on pulsed power is a brief summary of the information found in [2].

Pulsed power is used to discharge stored energy into a load in a single short pulse or short pulses with a controllable repetition rate. Important pulse shape parameters such as rise time, decay time, and full width at half maximum (FWHM) can be seen in Figure 2. The pulse rise time is defined as the time it takes the voltage to rise from 10% to 90%. The decay time is defined as the time it takes the voltage to fall from 90% to 10%. Pulse duration can be defined many ways, one of which is the FWHM or it could be the duration of 90% of the peak voltage. Another important requirement for some applications is the flatness of the plateau region.

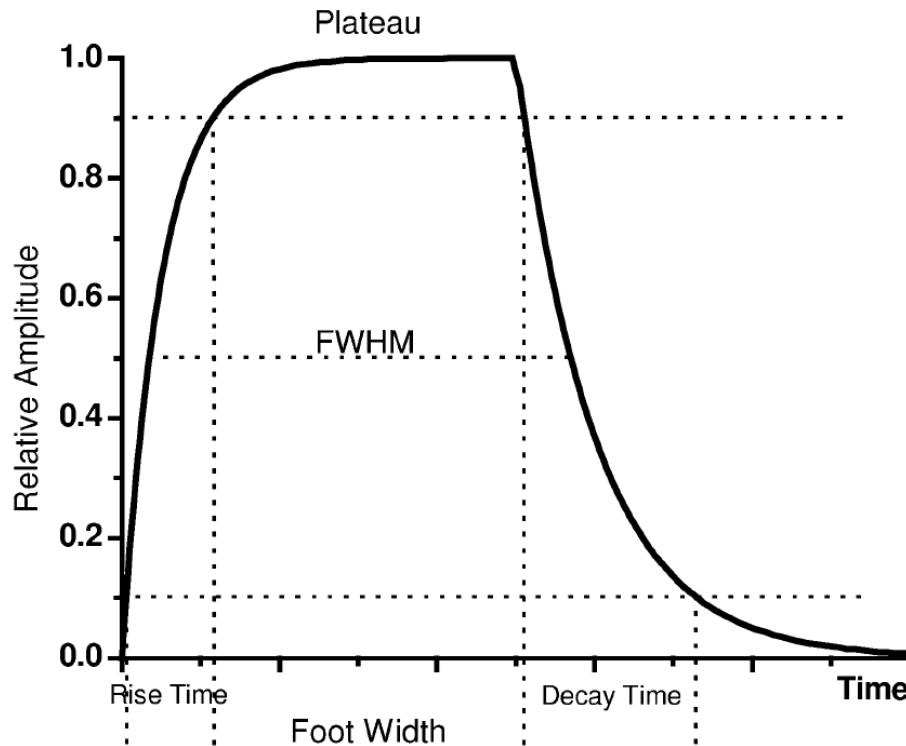


Figure 2 – Pulse Shape Parameters [2]

The general function of the production of the high power electrical pulses is always based on storing energy that is charged slowly at a relatively lower charging power and then discharging it rapidly by activating a switch. The discharge leads to a large power multiplication that can be scaled by repeating the process by adding multiple stages to the device. This process can also be used to shape the pulse by providing the required rise time, decay time, FWHM, etc.

There are two different ways to store electrical energy, either capacitively in an electric field or inductively in a magnetic field. The capacitive storage is

$$\omega_e = \frac{\varepsilon\varepsilon_0 E^2}{2} \quad (1)$$

where ε is the relative permittivity of the material in F/m, ε_0 is the permittivity of free space in F/m, E is the electric field density in V/m, and ω_e is the energy density stored in the electric field in kJ/m³. The inductive storage is

$$\omega_m = \frac{B^2}{2\mu\mu_0} \quad (2)$$

where μ is the relative permeability of the material in H/m, μ_0 is the permeability of free space in H/m, B is the magnetic field strength in T, and ω_m is the energy density stored in the magnetic field in MJ/m³. Typical values of ω_e are 10-80 kJ/m³ and typical values of ω_m are 1-50 MJ/m³ so the energy density stored in a magnetic field is about two orders of magnitude higher than the energy density stored in an electric field. The value of ω_e is dictated by the breakdown strength of the material while the value of ω_m is limited by the onset of melting at the conductor surface.

The generation of pulses using capacitive storage requires one or more closing switches that remain open during the charging of the energy store. The switches are then closed and the power amplification is achieved through current amplification. The generation of pulses using inductive storage requires an opening switch that remains closed during the charging of the energy store. The switch is then opened and the power amplification is achieved through voltage amplification. Even though inductive storage has higher energy

densities, capacitive storage is used more often because it is easier to design and build closing switches.

An advantage to pulse power is that it has a very high peak to average power ratio. This allows for the ability to use threshold and nonlinear effects as well as suppress competing heating processes. The short pulse duration is another advantage to pulse power, and it allows for the ability to exploit the time domain or to avoid competing processes.

Military requirements for pulsed power based weapons and simulation and diagnostic tools have been the main driving force behind the development of pulsed power. This includes efforts undertaken to develop high power microwave weapons. As the components, such as high voltage capacitors and high power semiconductor switches, become more reliable and cheaper new interest has been generated in commercial and industrial purposes. [2]

2.3 Switches

The rise time, shape, and amplitude of the output pulse are strongly dependant on the properties of the switch. Closing switches are required for capacitive storage devices so those will be discussed first. Closing switches operate by a voltage breakdown across an element that was initially insulating. The voltage breakdown can be initiated externally by a trigger pulse or it can occur automatically as a result of an overvoltage. First gas

switches will be discussed, followed by semiconductor switches, and then finally magnetic switches. The switch information is a summary from [2].

2.3.1 Gas Switches

The first type of closing switch that will be discussed is gas switches. Gas switches are commonly used in high power pulse generators because they are easy to use, can handle very large currents and charges, and they can be triggered precisely. The method used to trigger the switch has a large influence on the ignition delay and its variance.

The operation of the switch can be divided into four phases: trigger phase, transition phase, stationary phase, and recovery phase. The trigger phase is the phase where there is a buildup of a trigger discharge. The transition phase, also known as commutation, is the transition from high impedance to low impedance in the switch. The stationary phase is when the switch is closed and has a constant conductivity. The recovery phase is where the previous electric field strength is restored.

2.3.1.1 Spark Gap

The first type of gas switch to be discussed will be the gas filled spark gap which can be seen in Figure 3. The spark gap has two methods of breaking down. The breakdown can occur either because its breakdown voltage has been exceeded or because the breakdown strength has been reduced by UV radiation, plasma diffusion, or some other event inside the spark gap.

Important design parameters of a spark gap include the self breakdown voltage and the variance of the breakdown voltage, which determines the probability of prebreakdown. Also important is the range of voltages that can be reliably triggered with sufficiently low prebreakdown probability, known as the operation range. Jitter, or the time variance of ignition, is another important variable. The switching time, prebreakdown inductance and capacitance, repetition rate capability, and lifetime and cost also have to be considered.

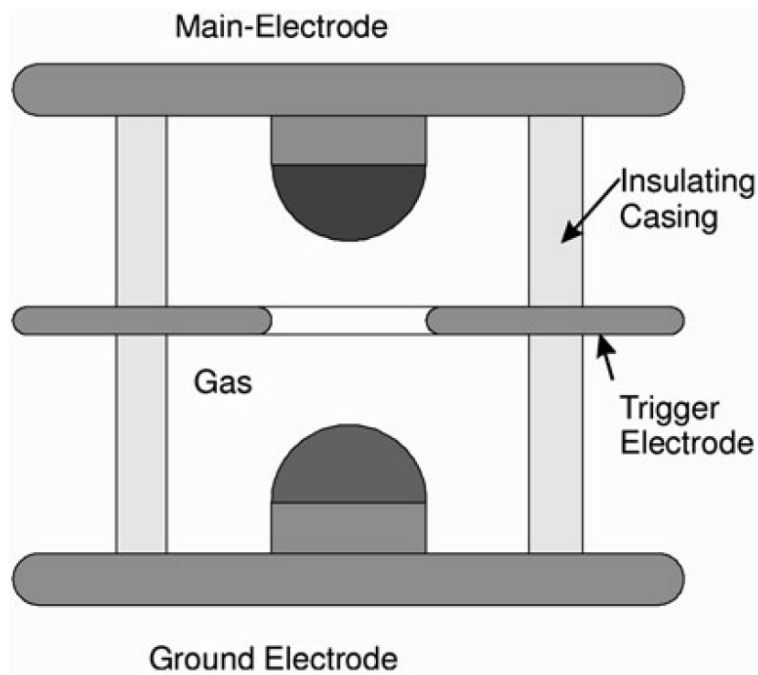


Figure 3 – Three Electrode Spark Gap [2]

2.3.1.2 Thyatron

Thyatronns are another type of gas switch. Thyatronns are gas filled switching devices, however unlike the spark gaps, their operating gas pressure is much lower. The thyatron allows the passage of large currents without significant electrode erosion through the presence of a plasma.

The thyatron uses a thermal electron source which is an advantage in that the hot cathode doesn't have a potential drop. A cold cathode requires a potential drop to accelerate the ions towards the cathode for secondary electron production. These energetic ions lead to erosion of the cathode and a limited lifetime, however, this can be mitigated by using a baffle to prevent the fast electrons from reaching the anode and causing damage. Current thyatronns can reach lifetimes of 10^5 operating hours at repetition rates of a few kilohertz and an average operating power at the megawatt level.

2.3.1.3 Krytron

The last type of gas switch to be discussed is the krytron. The krytron is a low pressure gas discharge device with a cold cathode. Krytrons have a short trigger delay time of about 30ns due to an already existing plasma created by a glow discharge between a keep alive electrode and the cathode. The current and voltages rise times are below 1ns. The maximum switching current is 3 kA and the maximum switching voltage is 8 kV. Pulse lengths can be up to 10 μ s and repetition rates of 1 kHz are achievable. The lifetime is limited to approximately 10^6 discharges.

2.3.2 Semiconductor Switches

Next semiconductor closing switches will be discussed. The limiting factors of a semiconductor device are associated with the low mobility and density of charge carriers in the plasma and the low operating temperature. Therefore, a large conducting region volume is required to conduct large currents.

2.3.2.1 Thyristor

The thyristor will be the first semiconductor switch discussed. Thyristors can operate at maximum voltages of 10 kV and peak currents of 30 kA. The maximum current rise time can be 20 kA/ μ s with a repetition rate of 10-50 Hz. High voltage high current thyristor stacks are highly complex and large in size which leads to a high production cost. These drawbacks have prevented their broad use in pulse power applications.

2.3.2.2 Insulated Gate Bipolar Transistor

Insulated gate bipolar transistors (IGBT) are another type of semiconductor closing switch. The IGBT combines the low resistance in the on state of a bipolar transistor with the loss free gate control of a field effect transistor. IGBTs have switch on times of the order of 10 ns, however they have lower current capabilities than thyristors. IGBTs can operate at maximum voltages of 4 kV and peak currents of 3 kA. Like thyristors they are complex and expensive so they have not been used widely in pulsed power applications.

2.3.3 Magnetic Switches

Magnetic switches, also known as saturable inductors, are based on the saturation of a ferromagnetic core. The magnetic switch is a passive switch unlike a thyatron or thyristor, which are both active switches. These magnetic switches operate with small losses and without wear. The ferromagnetic core of the magnetic switch begins with a high inductance while the capacitor is being charged. When the core saturates the inductance drops abruptly and the switch closes. A magnetic switch utilizes the complete range of the hysteresis curve from remanence to saturation. The hysteresis loop should approximate a rectangular form with an abrupt change of inductance of several orders of magnitude at saturation for fast and distinct performance of the switch.

The advantages of a magnetic switch are their wear free operation due to not having moving parts and their short recovery time. Their disadvantages include the inability to produce an ideal rectangular pulse. Due to leakage current there can be a long lasting foot preceding the main part of the pulse. [2]

2.3.4 Switch Summary

As can be seen below in Table 1 when the requirements for a system are on the gigawatts scale of power then the only two viable options are the spark gap and the magnetic switch. A magnetic switch is desirable over the spark gap due to its predictable triggering and its longer life due to the lack of moving parts. The spark gap has been thoroughly investigated and has a known output signature. The magnetic switch has not been investigated as thoroughly and needs a predictable output signature.

Table 1 - Comparison of Switch Characteristics [2]

Type	Maximum Voltage (kV)	Peak Current (kA)	Repetition Rate (Hz)	Lifetime (# of pulses)
Spark Gap	1-6000	10^{-3} -1000	1-10	10^3 - 10^7
Thyratron	5-50	0.1-10	1000	10^7 - 10^8
Krytron	8	3	<1000	10^7
Thyristor	<5	<5	10	10^8
IGBT	<4	3	100	10^8
Magnetic Switch	1000	100-1000	10	10^8 - 10^9

2.4 MPC Circuits

MPC circuits are used in applications that require high average power and high repetition rates. One important issue in these applications is the stability of the output pulse of the system. To understand magnetic compression systems there must first be an understanding of a hysteresis curve and how it functions. Then there will be a detailed discussion of how the system operates. This will be followed by detailing the timing variations in the system and some of the causes of those timing variations.

The advantages of MPC circuits are that they are passive and require a low current first stage switch. This ability to use a low current low voltage switch leads to increased reliability and robustness because high current high voltage switches are inherently unreliable. The reliability and robustness allows for the MPC circuits to be easily adapted for high repetition rates for high average power applications. [3]

Some other disadvantages of the MPC circuit are there is no ‘off the shelf’ design of saturable inductors, core demagnetization is needed, the system must be designed to match the load to prevent reflections, and the pulse width is not adjustable. [4]

2.4.1 Hysteresis

A B-H hysteresis curve shows the relationship between the magnetic flux density, B, and the magnetic field intensity, H. An example of a hysteresis curve can be seen below in Figure 4. The explanation of how the hysteresis curve behaves is a summary from [5].

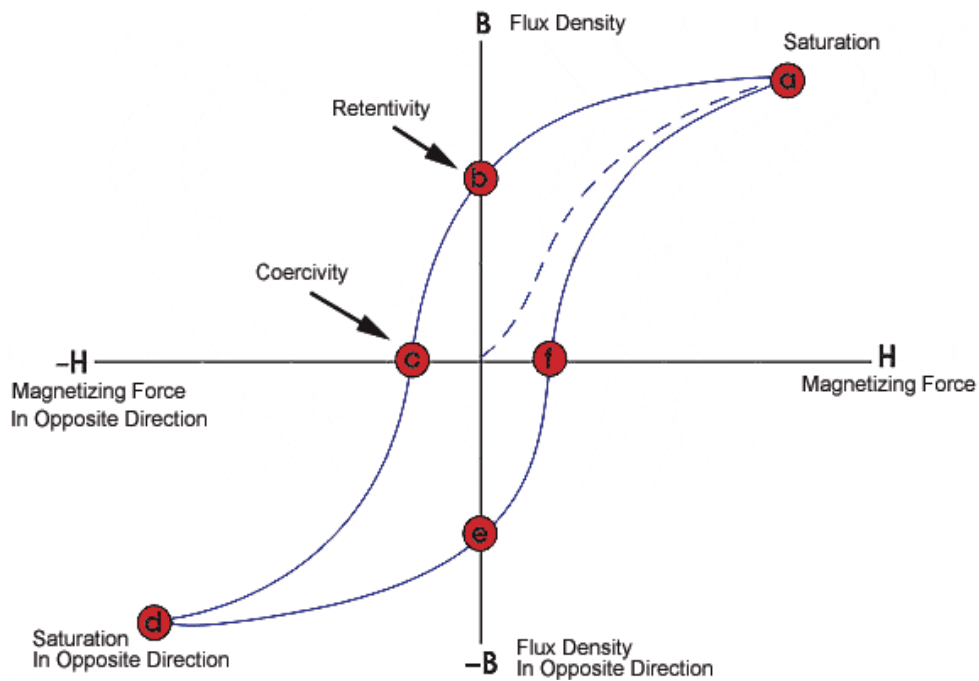


Figure 4 – Magnetic Core B-H Curve [5]

To determine the hysteresis curve of a ferromagnetic material, the magnetic field intensity is varied while the magnetic flux density is measured. If the ferromagnetic material has never been magnetized or the material has been demagnetized then it will

begin at the origin on Figure 4. As magnetic field is increased the material will follow the dashed line towards the saturation point at a. At this point almost all of the magnetic domains are aligned and an additional increase in the magnetizing force will produce very little increase in magnetic flux and saturation has been achieved.

When the magnetic field intensity is reduced to zero, the curve will move from saturation to point b. Point b is called the retentivity point because even though the magnetic field has been reduced to zero it still retains some of its magnetic flux. This means that some of the magnetic domains in the material have lost their alignment but others have remained aligned.

As the magnetizing current is reversed, the curve moves to coercivity at point c, where the flux has been reduced to zero. This is the point where enough of the domains in the material have been flipped by the reverse magnetizing current that the net flux is zero. The force required to remove the residual magnetism from the material is called the coercive force or coercivity of the material.

As the negative magnetizing current is increased, the material will move towards point d and become saturated in the opposite direction. When the magnetic field intensity is reduced to zero, the curve will move from reverse saturation to point e. Point e is the point where even though the magnetic field has been reduced to zero it still retains some of its magnetic flux.

If the magnetizing current is applied in the positive direction then the flux density will return to zero at point f. Notice that the curve did not return to the origin of the graph because some force is required to remove the residual magnetism. The curve will take a different path from point f back to the saturation point where it will complete the loop.

The hysteresis curve can be used to determine a number of magnetic properties. These include retentivity which is the value of the magnetic flux of a material when the magnetic field is removed after achieving saturation. Also residual magnetism can be determined. This is the magnetic flux density that remains in a material when the magnetizing current is zero. Residual magnetism and retentivity are the same when the material has been magnetized to the saturation point. However, the level of residual magnetism may be lower than the retentivity value when the magnetizing force did not reach the saturation level.

In addition coercive force can be determined. Coercive force is the amount of reverse magnetic field which must be applied to a magnetic material to make the magnetic flux return to zero. Permeability, μ , can also be determined. Permeability is a property of a material that describes the ease with which a magnetic flux is established in the component. And finally reluctance can be determined. Reluctance is the opposition that a ferromagnetic material shows to the establishment of a magnetic field. Reluctance is analogous to the resistance in an electrical circuit. [5]

The slope of a line on Figure 4 is permeability, μ , defined by

$$\mu = \frac{B}{H}. \quad (3)$$

The area enclosed by the hysteresis curve is energy loss. The area between the hysteresis curve and the vertical axis is recoverable stored energy defined as

$$\frac{W}{m^3} = \int BdH. [6] \quad (4)$$

The total flux, ϕ , through the entire cross-sectional area of the core, A_e is

$$\phi = B \cdot A_e. \quad (5)$$

The total magnetic force, F , around the entire magnetic path length of the core, l_e is

$$F = H \cdot l_e. \quad (6)$$

The permeance, P , can be calculated by

$$P = \frac{\phi}{F} = \frac{\mu A_e}{l_e} \quad (7)$$

and is defined as the inductance of one turn wound on the core. [6]

To change the operating point in Figure 4 requires a change in energy. Faraday's Law

$$\frac{d\phi}{dt} = -\frac{E}{N} \quad (8)$$

and

$$\phi = \frac{1}{N} \int E dt \quad (9)$$

as well as Ampere's Law

$$NI = \int H dl \quad (10)$$

dictate the electrical to magnetic relationship. The flux change is governed by the voltage applied to the winding according to Faraday's Law. [6]

2.4.2 Operation

The MPC circuit, also known as a Melville line, uses capacitors and saturable inductors to compress the width of an applied pulse and can be seen in Figure 5. This compression substantially increases the peak power of the initially applied pulse while decreasing the elapsed time of the pulse.

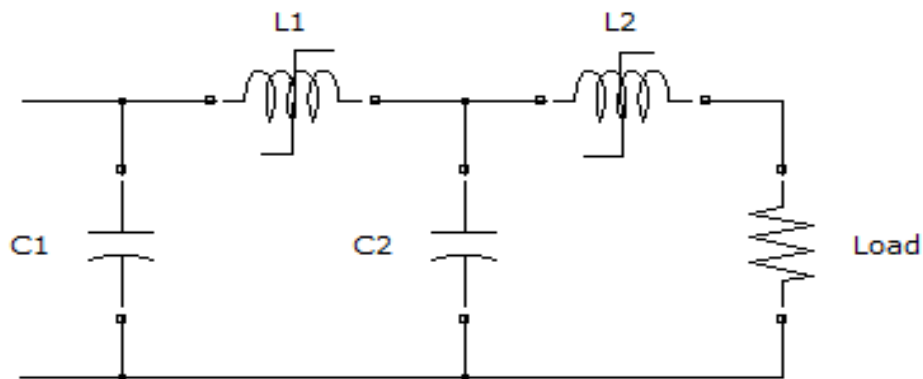


Figure 5 – Two Stage MPC Circuit

In a MPC circuit the capacitors are chosen to be equal in order to have complete charge transfer. Since the energy in the pulse remains the same if you ignore losses, and then when the pulse becomes shorter the peak power must increase. [4]

The MPC circuit operates by increasing the magnetic field, B , on an inductor such that it saturates the inductor. The magnetic field is proportional to the time integral of the voltage across the inductor, also known as the volt-second product.

As the voltage on C_1 increases, the magnetic field in the inductor traverses from an initial state, represented as 1 in Figure 6, through the path 1-2-3-4. This would be beginning at the saturation in the negative direction, point d in Figure 4, and moving through points e and f. If the stage is properly designed, the core of the inductor will transition from 4 to 5 close to the peak voltage on C_1 . The transition from 4 to 5 signifies the saturation of the inductor and causes the inductance and therefore the impedance to be reduced significantly. This saturation will cause C_1 to discharge into C_2 at a much faster rate than C_1 was charged which will lead to a compressed pulse and an increased peak power. This behavior resembles the characteristics of a switch so the saturable inductor is often called a magnetic switch. The MPC circuit must then have a reset circuit to apply a reverse current to the magnetic switch to return it from point 5 through 6 and return to 1 so it will be passing through its retentivity point, coercivity point, and back to negative saturation. [3]

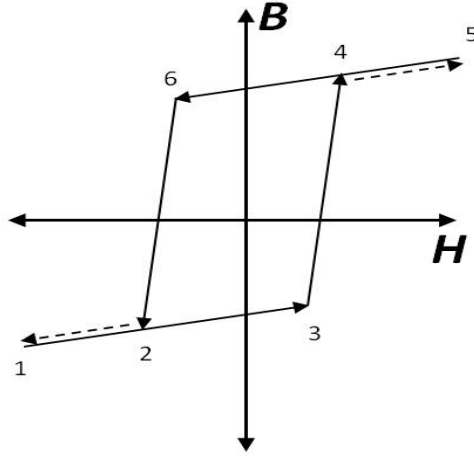


Figure 6 – Hysteresis Behavior of the Core of a Saturable Inductor [3]

The pulse compression rate ratio, κ , of stage n can be defined as

$$\kappa = \frac{\tau_n}{\tau_{n+1}} = \sqrt{\frac{L_{nu}}{L_{ns}}} \quad (11)$$

where τ_n is the pulse rise time of stage n , τ_{n+1} is the rise time of stage $n+1$, L_{nu} is the unsaturated inductance of stage n , and L_{ns} is the saturated inductance of stage n . [4]

The unsaturated inductance, L_u , of a ring shaped solenoid is

$$L_u = \frac{\mu_0 \mu_{ru} AN^2}{l} \quad (12)$$

where μ_0 is the permeability of free space, μ_{ru} is the unsaturated relative permeability, A is the magnetic material cross section area, N is the number of conductor turns, and l is the magnetic field path length. The saturated inductance, L_s , of the same ring shaped solenoid is

$$L_s = \frac{\mu_0 \mu_{rs} AN^2}{l} \quad (13)$$

where μ_{rs} is the saturated relative permeability. This provides a ratio of unsaturated inductance versus saturated inductance of

$$\frac{L_u}{L_s} = \frac{\mu_{ru}}{\mu_{rs}} \quad (14)$$

Typical values for μ_{ru} are on the order of thousands to tens of thousands and typical values of μ_{rs} are approximately one. This will lead to a ratio of L_u to L_s on the order of thousands to tens of thousands. The switching of the saturable inductor uses the large ratio of the inductances to perform its function. [7]

The relationship between the voltage-time product and the flux density is

$$\frac{1}{N} \int_0^{T_s} V(t) dt = A_m \Delta B \quad (15)$$

where T_s is the time to saturation, $V(t)$ is the applied voltage, ΔB is the change in magnetic flux density, N is the number of conductor turns, and A_m is the magnetic material cross section area. [7]

2.4.3 Timing Variations

The jitter and timing transients that can manifest themselves in MPC circuits can be a problem. Precise analysis and design of the MPC circuit can be difficult because of the nonlinear characteristics of the magnetic switches. There are several sources for these

timing issues. One cause of the variations is that the volt-second product presented to each core must be regulated. Irregularities in the volt-second product can be caused by imperfections in the power supply providing the input pulses. The second cause of the variations is energy reflections due to mismatches between the stages of the system. The third cause is that the inductor doesn't return to point 1 on the B-H plane before each pulse is applied. The reset circuit connected to the inductors to reset the state of the inductor to point 1 is a low voltage power supply that is isolated from the pulse undergoing compression. [3]

The isolation between the reset circuit and the Melville line is never absolute. The complex interactions in the residual energy in the two systems will overcome the reset circuit's ability to reset the inductor to point 1 and will lead to a more complex path to be taken on the B-H hysteresis curve. These interactions will lead to timing variations on the pulse arrival at the output due to the variations in the starting point of the B-H curve of the inductor. [3]

Minimizing shot-to-shot and burst-to-burst pulse amplitude and timing variations is a key consideration for MPC circuits. As can be seen in Figure 7, scientists at Lawrence Livermore National Laboratories (LLNL) have done work to measure the timing variations in a MPC circuit. These variations are measured data particular to the system they have at LLNL. As can be seen there are variations in the pattern of the timing signature based on the pulse repetition frequency (PRF). The top part of Figure 7 is for a pulse repetition frequency (PRF) of 1 kHz. The pulse timing has some random jitter in it

but it also increases slightly before it starts a decreasing trend. All of the pulses were within 30 ns for arrival time. The bottom part of Figure 7 is for a PRF of 5 kHz. The pulse timing for the 5 kHz has almost no random jitter and is on a steadily decreasing timing pattern. The arrival time starts at around 220 ns and decreases steadily till it is at approximately 20ns after 50 pulses. [8]

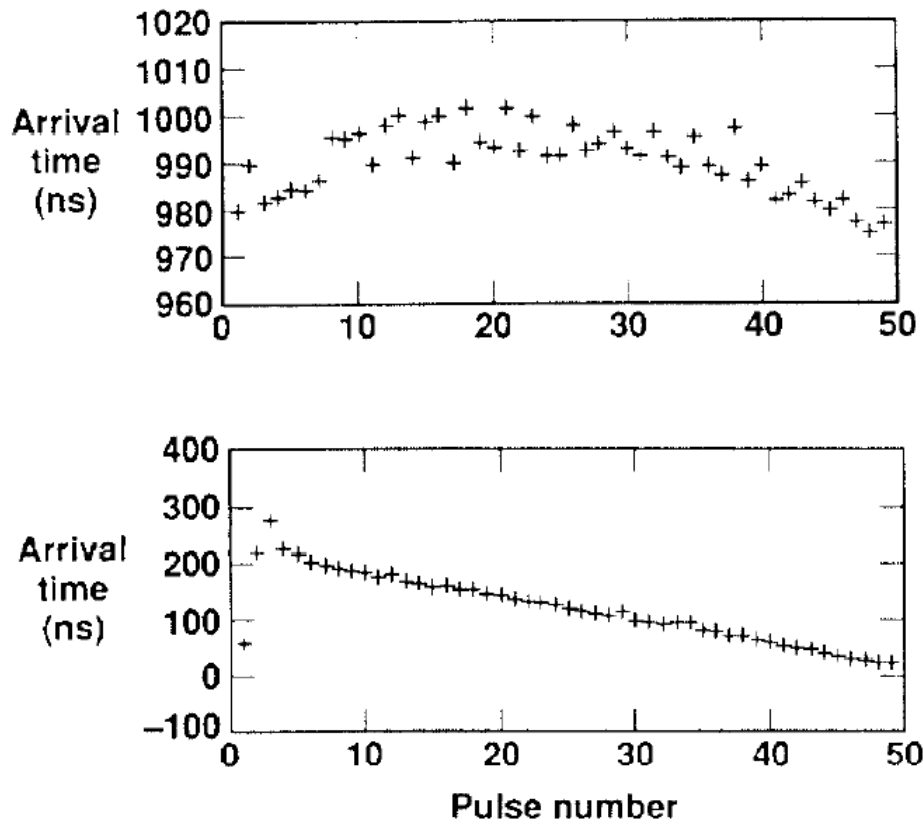


Figure 7 – Experimental Output Timing Signature of MPC Circuit used by LLNL for (top) 1 kHz PRF and (bottom) 5 kHz PRF [8]

2.5 Summary

As can be seen there has been previous work done on MPC circuits. There are even multiple examples of simulations being run to better understand the operations of the circuits. Only one of the sources has specifically looked at the repetition response, however, the information is for one specific system and is strictly experimentally collected data.

The papers from the scientists at Lawrence Livermore National Laboratories clearly illustrate that the magnetic switching in MPC circuits can introduce a timing variation. This variation is the focus of the simulation efforts that were done to determine the output timing signature of the MPC circuit.

III. Methodology

3.1 Chapter Overview

This chapter will begin with a discussion of the how the model was constructed. The discussion begins with a summary of [9] upon which the model is based. The chapter then goes into a discussion of how both the nonlinear inductor and the nonlinear resistor were created in Simulink. Finally discussed is how the circuit was laid out in Simulink and what the parameters were of that circuit.

3.2 Constructing the Model

MATLAB Simulink was the program used to model the circuit. Using the information provided in [9]. The mathematical model to represent a hysteresis curve is constructed using two monotonically increasing functions. Using this method the hysteresis curve can be simulated and will also exhibit important hysteresis properties such as minor loops. The mathematical model is able to be represented by a circuit model consisting of a nonlinear inductor and a nonlinear resistor in parallel. The data shown in Figure 8 and Figure 9 from [9] was then used as the functions for the nonlinear inductor and nonlinear resistor to create the hysteresis curve shown in Figure 10.

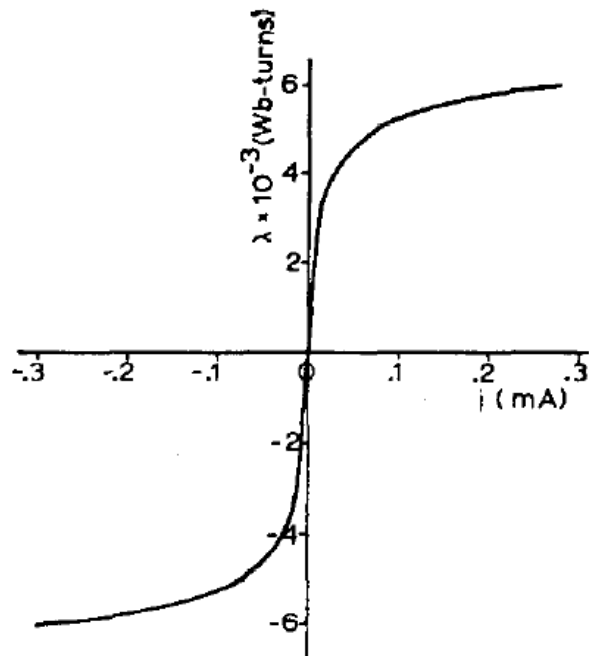


Figure 8 – Nonlinear Inductor Current versus Flux Curve [9]

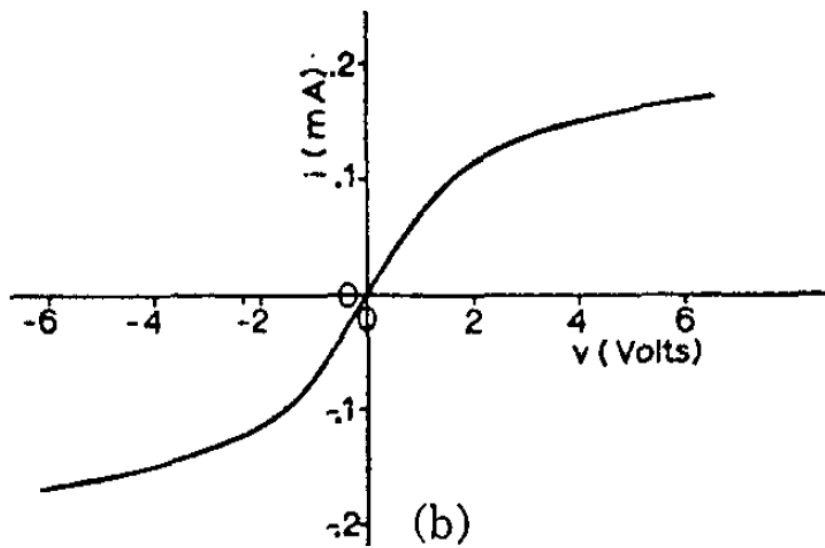


Figure 9 – Nonlinear Resistor Voltage versus Current Curve [9]

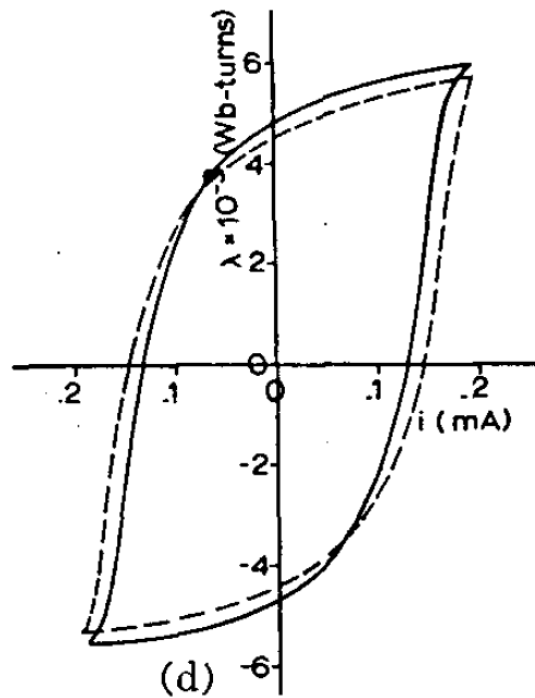


Figure 10 – Hysteresis Curve Corresponding to the Nonlinear Inductor and Nonlinear Resistor Provided in Figure 8 and Figure 9 [9]

Figure 8 shows the behavior of the nonlinear inductor as a function of the current and flux. As can be seen no current flows through the inductor until a threshold flux has been reached. Once this flux threshold has been reached the current then flows through almost unimpeded.

3.2.1 *Nonlinear Inductor*

The schematic for the nonlinear inductor subsystem can be seen in Figure 11. To construct the nonlinear inductor the first thing to do was recreate the inductor characteristics shown in Figure 8 for the i - λ curve. This was done by using a lookup table in Simulink and entering in the correct values for the table.

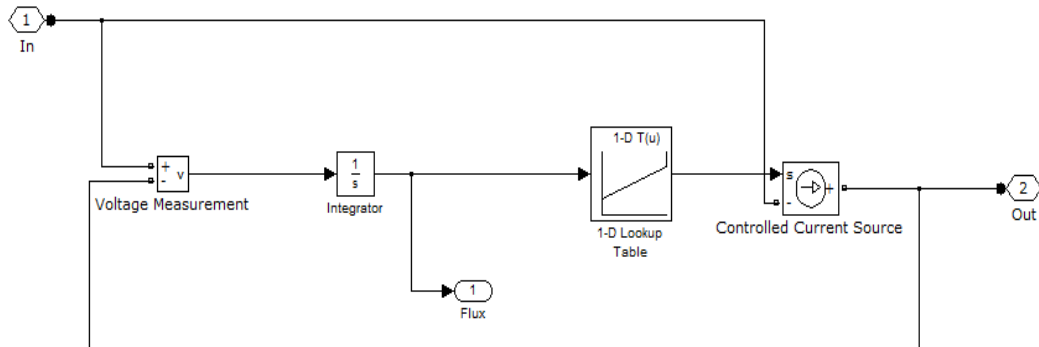


Figure 11 – Nonlinear Inductor Schematic in Simulink

To calculate the values the first thing that must be done is to calculate the flux at the breakpoint. The breakpoint is the point in Figure 8 where the slope of the line changes and signifies the transition from the unsaturated region to the saturated region. The breakpoint was estimated to occur at 0.05 mA. Since the circuit being used was using 120 V input for 0.01 s the flux can be calculated to be 1.2 V·s using

$$\Psi = \int V dt \quad (16)$$

where Ψ is the flux in the inductor and V is the voltage across the inductor. The 1.2 V·s can then be used in

$$i = \frac{\Psi}{L} \quad (17)$$

to determine the unsaturated inductance, L . Using the current at the breakpoint, 0.05 mA was used for i in Equation 17 and using the flux calculated before as 1.2 V·s this

produces an unsaturated inductance, L , of 24000 H. This unsaturated inductance is the slope of the line created by the flux and the current in the unsaturated region. To produce a saturated inductance that is close to zero, the breakpoint values on the lookup table had to be close to one to provide a slope of the saturated region that was close to zero and therefore approaching horizontal.

Once the lookup table was constructed, a subsystem was created in Simulink to provide the functionality of the nonlinear inductor. To determine the flux that is input to the nonlinear inductor the first thing that must be done is a voltage measurement. This is implemented in Simulink by using a Voltage Measurement block. The Voltage Measurement block determines the voltage across the nonlinear inductor subsystem. This voltage must then be integrated to obtain the flux. This is done in Simulink with an Integrator block. The Integrator block calculates the result from Equation 16 to determine the flux.

This flux was then used with the lookup table previously constructed. This was done by finding the flux value on the lookup table and determining the current that corresponded to that value. The value of the current from the table was then used as an input to a Controlled Current Source block in Simulink to output the correct current from the nonlinear inductor subsystem.

A mask was then created for the nonlinear inductor subsystem so that the important values of saturation flux, unsaturated inductance and the saturation characteristics could

be quickly changed to see how it affected the system. The mask can be seen in Figure 12 and the code used can be seen in Appendix A.

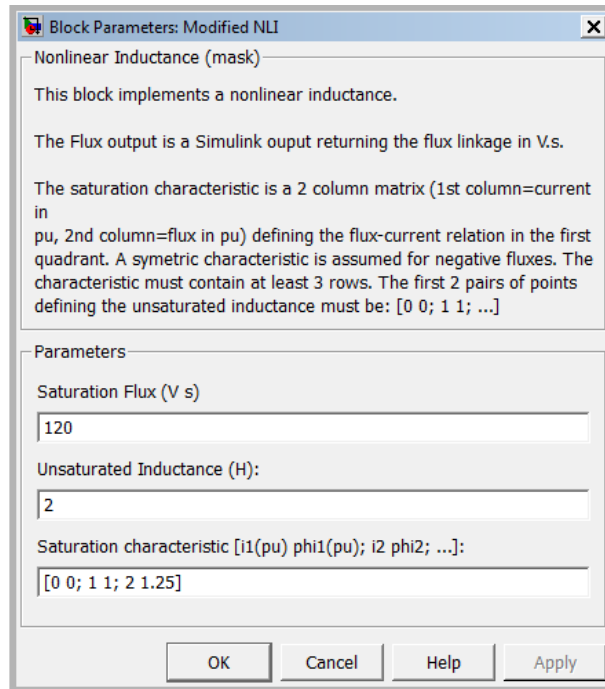


Figure 12 - Nonlinear Inductor Mask in Simulink

The saturation characteristics of the curve determine the slope of the saturated part of the inductor. This is done by changing the last two numbers in the list. The first numbers are always [0 0; 1 1] but the last two can be changed to adjust the slope. So for instance if you want the saturated inductance to be 25% of the unsaturated inductance you would make the saturation characteristics [0 0; 1 1; 2 1.25]. If you wanted the saturated inductance to be 0.01% of the unsaturated inductance then the saturation characteristics would be [0 0; 1 1; 2 1.0001]. The percentage is just the slope of the last part of the line so the rise over run of the last numbers, i.e.

$$\frac{1.0001-1}{2-1} = 0.0001 = 0.01\% \quad (18)$$

3.2.2 *Nonlinear Resistor*

The schematic for the nonlinear resistor can be seen in Figure 13. The first step in creating the nonlinear resistor was determining a function that could represent the $v-i$ curve seen in Figure 9. The atan function was determined to provide the best fit to the provided data. The function used was

$$i = A \cdot \text{atan}(x / B) \quad (19)$$

to create the desired curve. To determine the best shape of the function a MATLAB file was created where two variables, A and B , were varied to change the shape of the atan curve. The code of this file can be seen in Appendix B.

Once the curve had been recreated then a nonlinear resistor subsystem was created in SIMULINK. The first step in the subsystem calculates the voltage across the nonlinear resistor. This is then passed through a transfer function with a fast time constant of 0.01 μs to break the algebraic loop without changing the nonlinear characteristics. It is then sent through a Function block with properties of the atan function previously calculated. This block finds the voltage value on its x-axis and outputs the value of the corresponding current on the y-axis. The value provided is then used as an input in the Controlled Current Source block and output from the nonlinear resistor subsystem.

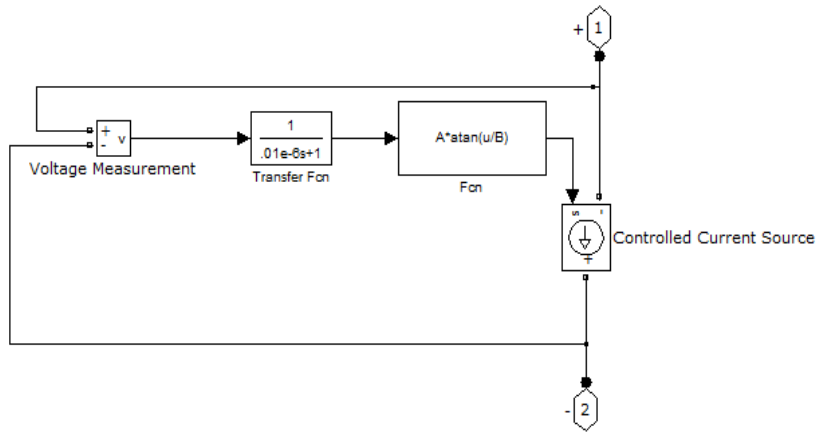


Figure 13 - Nonlinear Resistor Schematic in Simulink

A mask was then created for the nonlinear resistor so that the important values could be quickly changed. The mask can be seen in Figure 14. This mask allows for the two variables, A and B, used in the atan function to be changed quickly and easily.

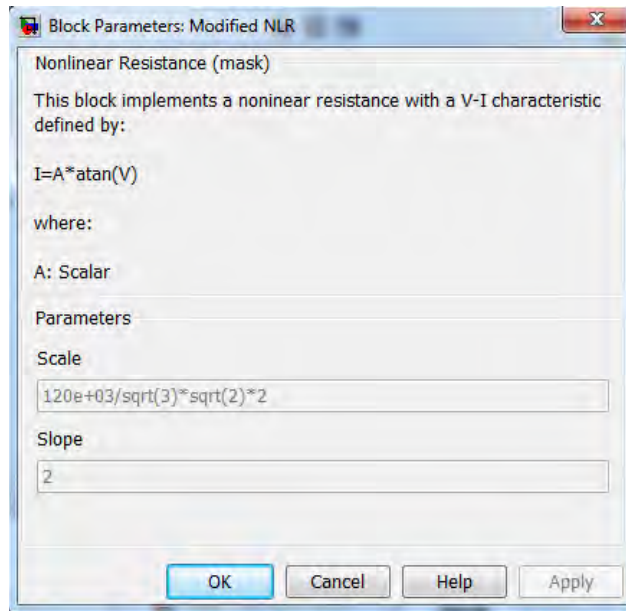


Figure 14 - Nonlinear Resistor Mask in Simulink

3.3 Circuit Parameters

These two devices were then used to model a saturable inductor and put into the circuit shown in Figure 15. The circuit is a basic layout of a MPC circuit.

The Pulse Generator block is producing a square pulse that is 0.01 s in duration every 1s starting at time 0.5 s with a magnitude of 120. This pulse generator then feeds into a Controlled Voltage Source block that converts this input signal into a voltage. This voltage is then fed into a capacitor C_1 that is 2 μF . Once the flux across the nonlinear inductor is high enough it saturates at which point it allows the current to flow through to the next capacitor C_2 . This discharge into C_2 happens in a shorter amount of time than C_1 was charged which provides the pulse compression. The value of C_2 is also 2 μF . C_2 then charges and once the flux is high enough across the second nonlinear inductor then it saturates and allows the current to flow into the load. The value of the load is 100 Ω .

To measure the currents in the system two Current Measurement blocks were added. The first Current Measurement block was put in the loop that the first saturable inductor is in. The second Current Measurement block was put in the loop that the second saturable inductor and the load are in. These two Current Measurement blocks were then attached to a Scope block so that the measurements could be seen and recorded.

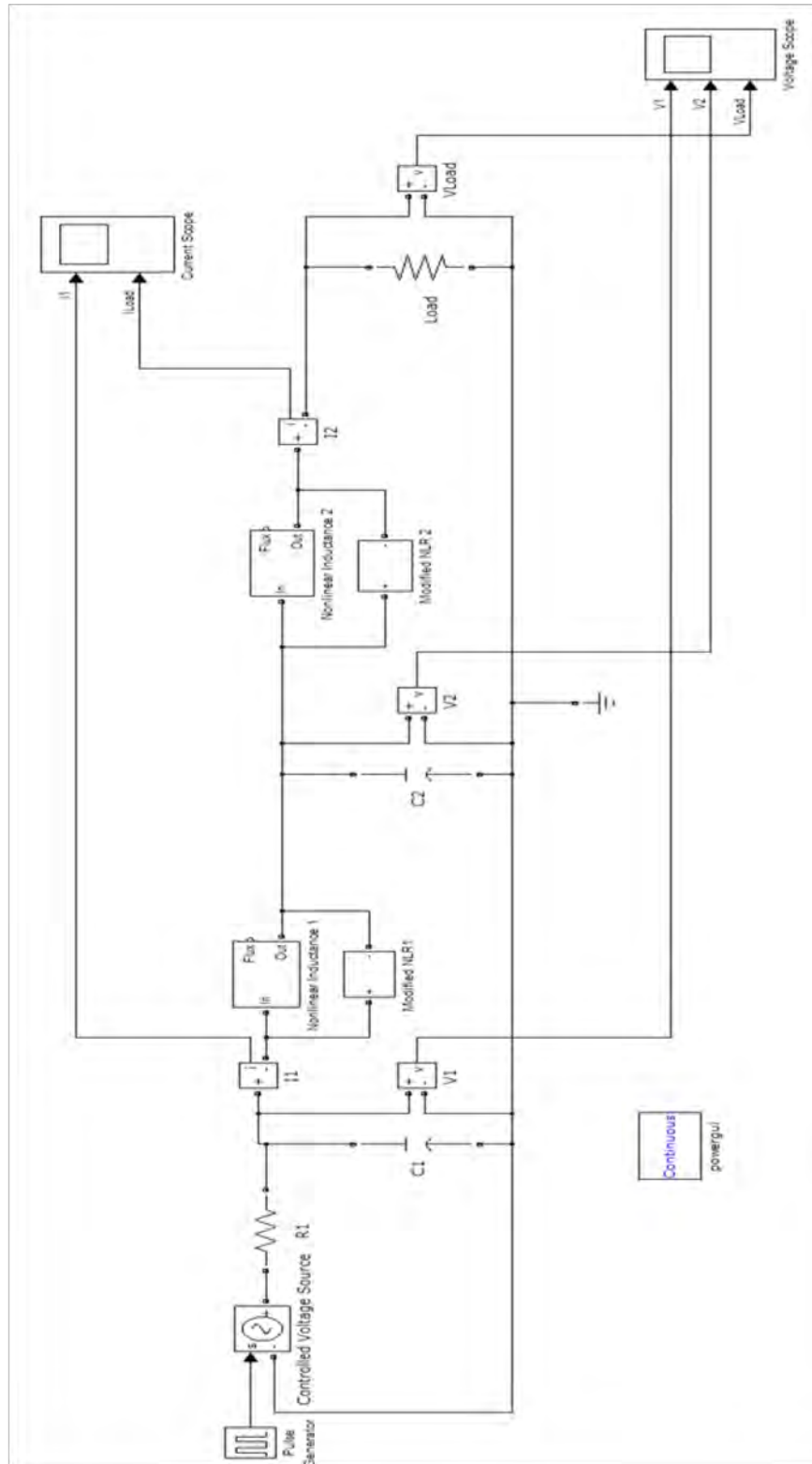


Figure 15 – Circuit Layout Used in Simulink for MPC Circuit Simulations

To measure the voltages in the system three Voltage Measurement blocks were added. The first Voltage Measurement block was put across C_1 . The second Voltage Measurement block was put across C_2 . The third Voltage Measurement block was put across C_3 . These three Voltage Measurement blocks were then attached to a Scope block so that the measurements could be seen and recorded.

3.4 Summary

This chapter began with an analysis of the [9] to determine a way to model the saturable inductors needed for the MPC circuit. The values used in the paper were then used to construct a nonlinear inductor and a nonlinear resistor to properly model the hysteresis behavior of the saturable inductor. The nonlinear inductor and nonlinear resistor were then put in parallel in a MPC circuit to model the timing signature. This timing signature as well as a validation of the circuit will be discussed in the next chapter.

IV. Analysis and Results

4.1 Chapter Overview

First the output pulse forms of the simulations are presented. To trust these results it must first be validated, therefore the next part of this chapter will be a discussion on how the validation was done. Finally there will be the presentation of the signature of the MPC circuit and an explanation on why the simulation produced the results seen.

4.2 Simulation Results

The results of the first simulation can be seen below. This simulation was performed with the parameters outlined above for the circuit shown in Figure 15. Figure 16 shows the voltage pulse data for the entire 10 s simulation run. The top plot is the input pulses into the MPC circuit every 1 s. The middle plot is the voltage across C_2 of the MPC circuit and the bottom plot is of the voltage across the load.

To provide more detail Figure 17 shows a zoomed in view of the first pulse at 0.5 s. On Figure 17 the input voltage of 120 V for 0.01 s can be seen in the top plot. In the middle plot it can be seen the point that L_1 switches closed just after 0.508 s and the voltage across C_2 . The bottom plot is of the voltage across the load of the MPC circuit and it can be seen when the second switch, L_2 , closes after 0.512 s and allows the discharge across the load.

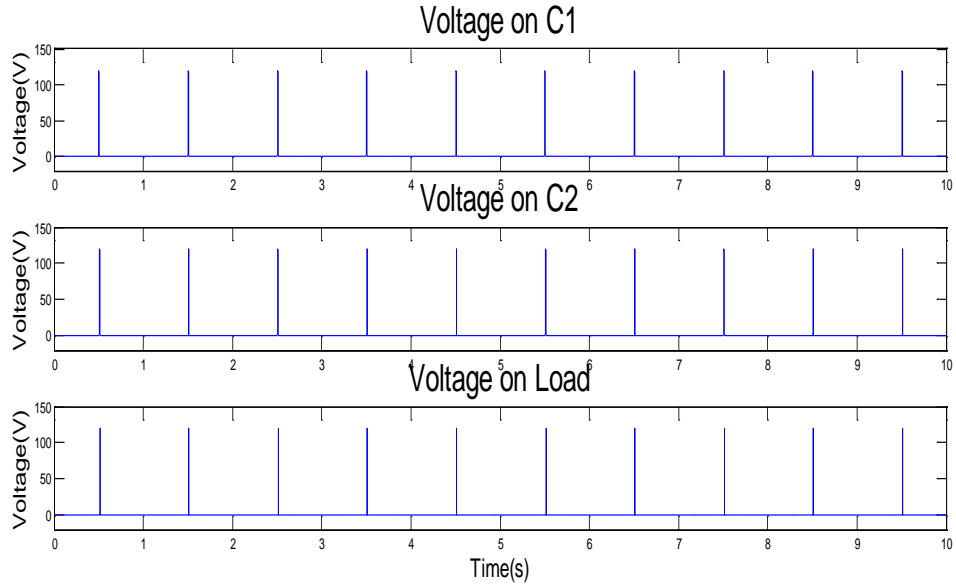


Figure 16 - Pulse Shape of the Voltage for a 10 s Simulation for (top) the Input Voltage, (middle) the Voltage across C_2 , and (bottom) the Voltage across the Load

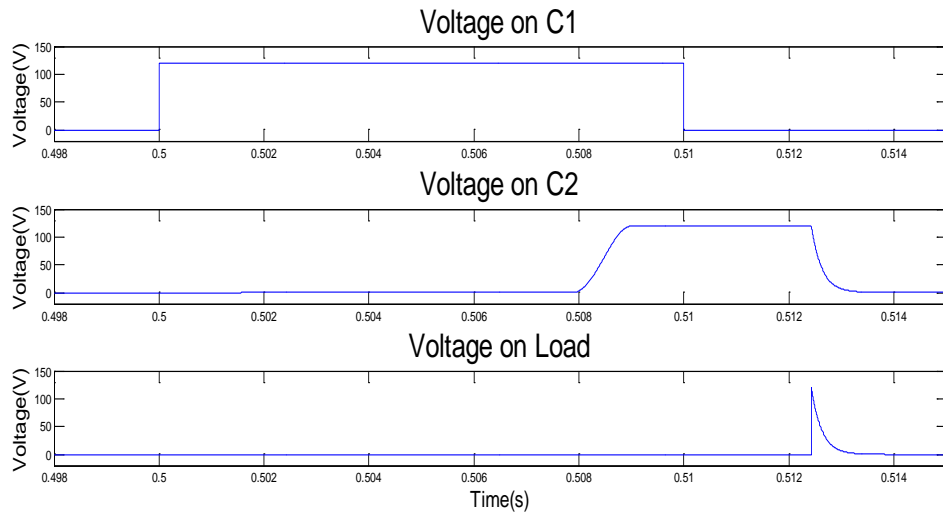


Figure 17 - Pulse Shape of the Voltage for a single Pulse for (top) the Input Voltage, (middle) the Voltage across C_2 , and (bottom) the Voltage across the Load

Next the form of the current pulses was evaluated. Figure 18 shows the current for the entire 10 s simulation run. The top plot is of the current through L_1 and the bottom plot is of the current through L_2 .

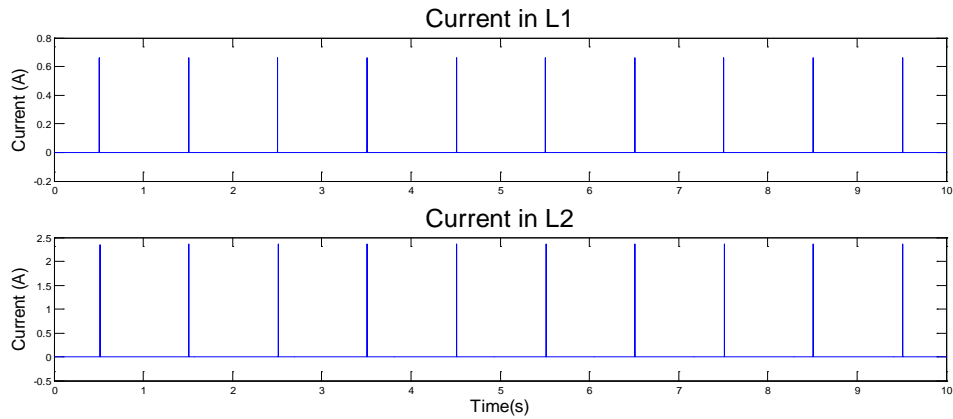


Figure 18 – Pulse for the Current for a 10 s Simulation for (top) the Current through L_1 and (bottom) the Current through L_2

Figure 19 shows the form of a single pulse. The top plot shows the current through L_1 in the MPC circuit. The bottom plot shows the current through L_2 in the MPC circuit.

From a comparison of the two currents it can be seen that the circuit is providing pulse compression. The current in the bottom plot is shorter in duration and also has a higher peak current.

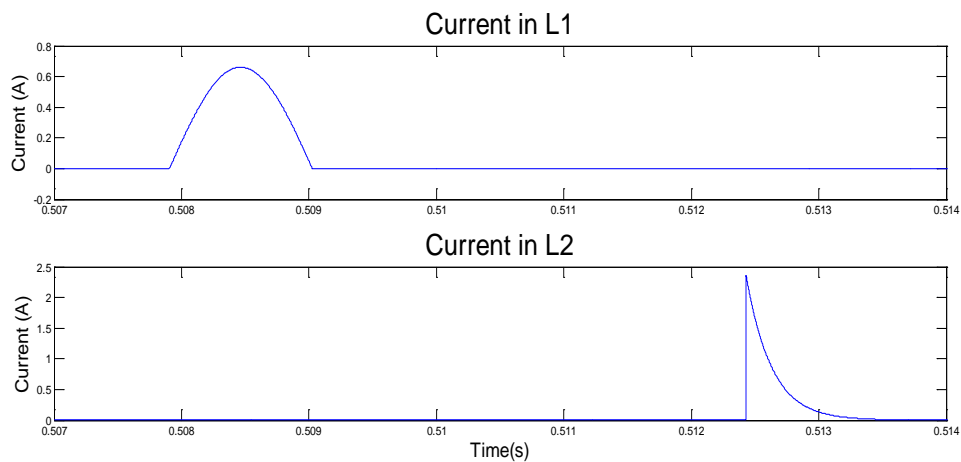


Figure 19 – Pulse Shape of the Current for a single Pulse for (top) the Current through L_1 and (bottom) the Current through L_2

The delay seen in Figure 19 between the current in L_1 and the current in the load is caused by the time it takes L_2 to switch. There is a time where the voltage on the capacitor C_2 is constant which means that no more current is flowing onto the capacitor.

This relationship is defined by

$$C = \frac{Q}{V} \quad (20)$$

where C is the capacitance, Q is the charge, and V is the voltage. Since

$$i = \frac{dQ}{dt} \quad (21)$$

if the voltage and capacitance aren't changing then no current can be flowing because the charge, Q , can't change either. As can be seen from Figure 17 the duration of the plateau of the maximum voltage on C_2 is the same as the delay between the two currents in Figure 19.

4.3 Validation of Circuit

To confirm the results of the circuit it was compared to theoretical data. Of particular importance was to make sure the circuit was behaving as it should in compressing the incoming signal. The theoretical circuit proposed by Melville can be seen in Figure 20. This can be compared to the representation of the circuit used in the modeling in the previous chapter which is provided in Figure 5. When comparing Melville's circuit to the one used in the modeling the current in P_2 of Melville's circuit is equivalent to the current in L_1 of the circuit used for the modeling. In addition the current in P_3 of Melville's circuit is equivalent to the current in L_2 of the circuit used for the modeling.

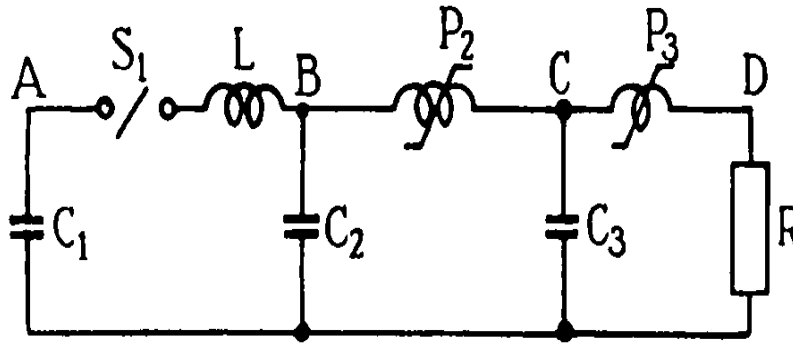


Figure 20 – MPC Circuit Proposed by Melville [10]

The next step to verify the results is to compare the currents of both Melville's circuit and the circuit used in the model. Melville's current can be seen in Figure 21 and the model's current can be seen in Figure 19. As can be seen by comparing Figure 21 and Figure 19 not only is it compressing the current and increasing its peak current but it even has the same shape. This confirms that the circuit modeled in the previous chapter is performing in the desired manner.

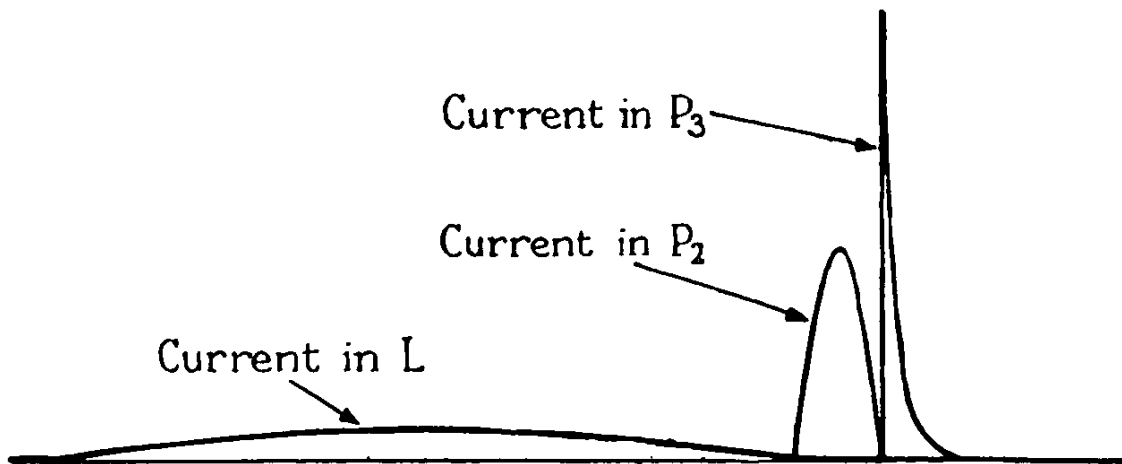


Figure 21 – Current Measurements of Melville's Circuit [10]

4.4 Timing Variation Signatures

After confirming the circuit model was producing the desired results the next step was to determine the pulse timing signature and the reason for the particular signature. The first step was to take the circuit laid out in the chapter above and run it for 10 s. This provided 10 pulses that could be measured. To calculate the pulse timing a MATLAB function was created. This function can be seen in Appendix C. What the function does is calculate the time between the initial pulse coming into the MPC circuit at C_1 and the pulse leaving the MPC circuit at the load. The data shown in Figure 22 is for a pulse every second that lasts for 0.01s. Since H is directly proportional to the flux, the farther the hysteresis curve must travel on the x axis the more flux that is required to close the magnetic switch which means it will take longer to switch provided the same flux.

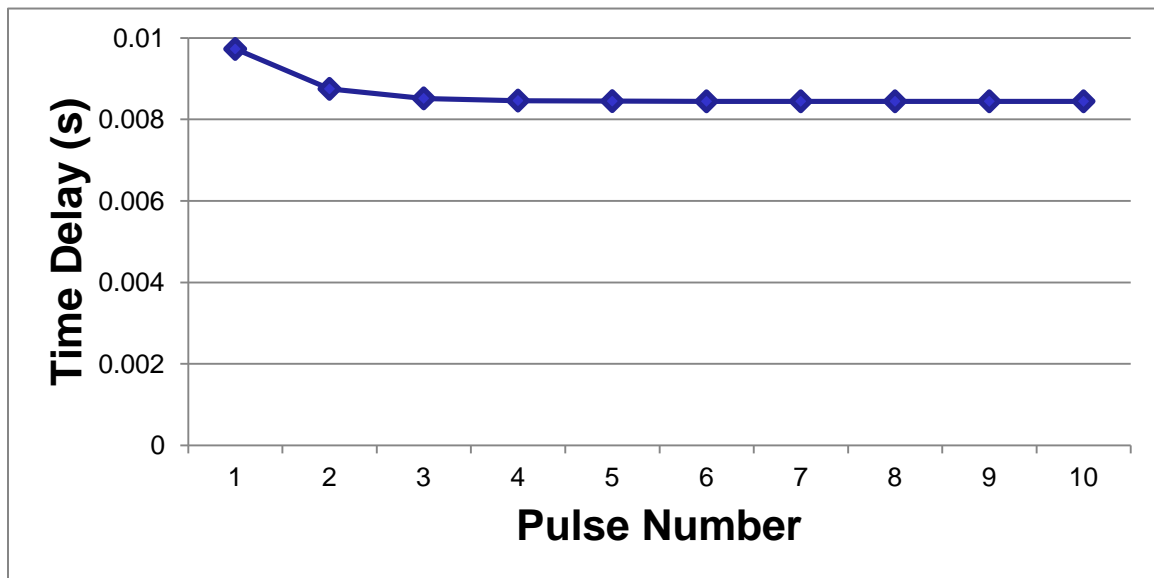


Figure 22 – Pulse Delay between the Input Pulse and the Output Pulse for a Square Pulse 0.01 s in duration every 1 s

As can be seen in Figure 22, the first pulse delay is 0.0097 s. Since the reset circuit was never able to function properly in the model, this would correspond to movement from the origin on Figure 4 to point a where the inductor would saturate. The core would then move towards point b in Figure 4 after the field is removed. Since there is no functioning reset circuit, it will never move past point b. Since the distance from where the inductor is currently back to a is shorter than from the origin to a the next pulse is faster. For the second pulse the curve doesn't get a chance to fall all the way back to the previous spot so the next pulse is even faster. After the second pulse, the hysteresis curve finds steady state in a minor loop and the delay time levels off at 0.0084 s.

The next step was to speed up the pulses entering the circuit. The same 0.01 s pulse was input into the MPC circuit however the time between the pulses was decreased to 0.1 s. This should lead to smaller time delays due to a shorter path on the hysteresis curve. The time delay curve of this can be seen in Figure 23.

As can be seen in Figure 23 the pulse time delay begins at the same 0.0097 s and has the same decaying shape that the previous simulation did but the time delay falls very rapidly and to a much shorter time. This validates the hypothesis that the time is so short that the inductor core is unable to reset to its initial starting point and is therefore creating a shorter path on the hysteresis curve.

To verify this, the same circuit was provided the same 0.01 s long pulse but this time every 10 s. If the theory is correct then it should lead to a flatter curve where the core is

able to reset to the initial starting point after every pulse so the path taken on the hysteresis curve will be the same. The results of this simulation can be seen in Figure 24.

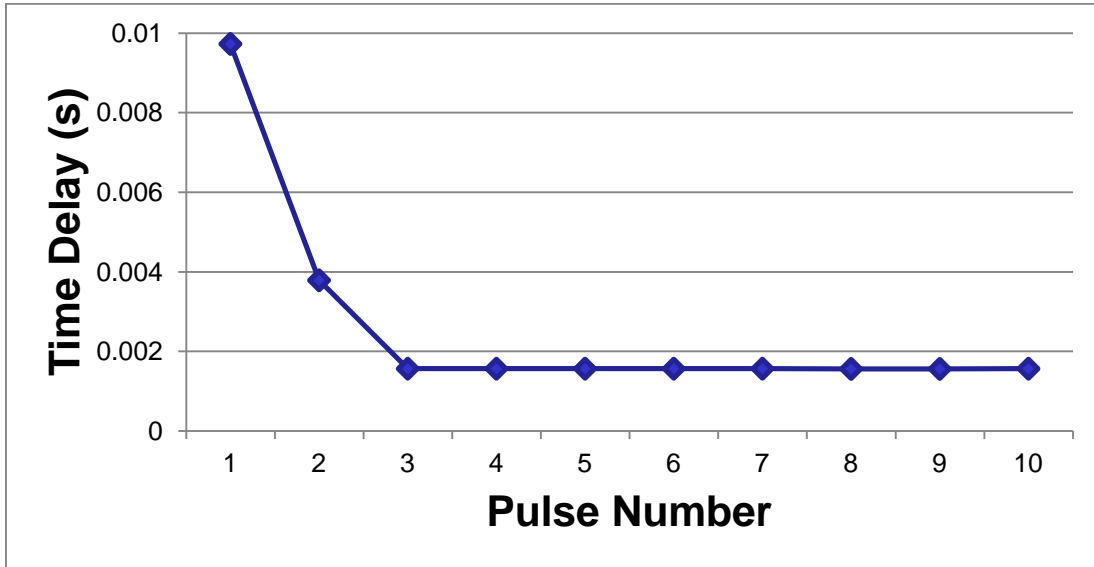


Figure 23 - Pulse Delay between the Input Pulse and the Output Pulse for a Square Pulse 0.01 s in duration every 0.1 s

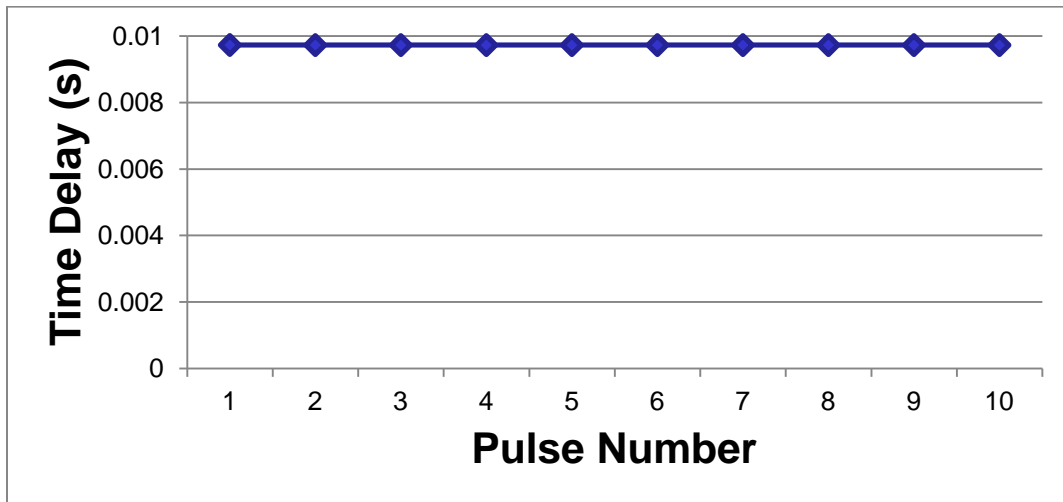


Figure 24 - Pulse Delay between the Input Pulse and the Output Pulse for a Square Pulse 0.01 s in duration every 10 s

As Figure 24 shows the pulse delay time begins at the same 0.0097 s but this time it never decays. This confirms that the saturable core is able to reset to the same point on the hysteresis curve after every pulse.

4.5 Summary

The first step was to verify that the circuit model was working as intended. To do this the simulation results were compared to the theoretical values proposed by Melville. After the results were verified the timing delay signatures of the model was examined. It started with examining the initial values of the circuit and then adjusting the times between pulses to collect data on the hysteresis curve behavior. The next chapter will be used to summarize the results of the research as well as suggest some future areas of work.

V. Conclusions and Recommendations

5.1 Chapter Overview

This chapter will bring about the conclusions of the research conducted earlier in the paper. Also discussed will be any recommendations for future work that can be done with this project.

5.2 Conclusions of Research

This thesis started with a brief introduction to HPM and the desire to model the signature of the MPC circuit. Before the modeling could be done an understanding of the underlying concepts first had to be developed. It began with a development of what pulsed power is and described some of the types of switches that could be used to create the pulsed power. Then magnetic switches were described in more detail. To achieve that a description of a hysteresis curve had to be provided so the behavior of the switch could be understood. Next an explanation of how the MPC circuit itself actually functions was given. This was followed by a discussion on the timing instabilities of the MPC circuit.

The next step was to build a model to conduct the simulations. This was done based on a paper by Chua and Stromsmoe. The paper detailed a way to simulate the properties of a hysteresis curve of a saturable inductor by putting a nonlinear inductor and a nonlinear resistor in parallel. For this to be done a nonlinear resistor and nonlinear inductor

subsystem had to be built in Simulink. These subsystems were then put into a circuit design and the simulations were run.

After the simulations were run the first step was to verify that the data being provided was the information desired and that it was accurate. To do this the output of the simulation was compared to data provided by the original creator of the circuit, W.S. Melville. After the data was compared and shown to verify the outputs then the pulse time delay signature could be evaluated.

The first step was to run the simulation exactly as it was initially designed with a 0.01 s pulse every 1 s. This produced a pattern very similar to a decaying exponential. This signified that the hysteresis curve wasn't able to reset to the same point after every pulse. Once a path had been achieved that it was able to reset to the same point every time then the curve leveled off.

After that the pulse speed of the simulation was sped up so that it was providing the same 0.01 s pulse but this time it was doing it every 0.1 s. This led to a decaying exponential shaped curve but it bottomed out at a much lower time delay. This indicated that the alternate path on the hysteresis curve created was much smaller than the initial path.

Finally the pulse speed of the simulation was slowed down so that it was providing a 0.01 s long pulse every 10 s. This led to a nearly flat time delay curve. This means that the

core of the inductor was able to nearly reset to its initial starting point after every pulse thus maintaining the initial hysteresis shape.

5.3 Recommendations for Future Research

The next major part of this project would be to design and implement a functioning reset circuit for the saturable inductors. This reset circuit would allow for the initial state of the hysteresis curve to be set at point 1 in Figure 6. It would also allow for the hysteresis curve to be reset past point b in Figure 4. If not given enough time to reset all the way to the starting point at 1 even with a reset circuit the time delay will still have a decaying shape. However if given enough time between pulses and a large enough current in the reset circuit, potentially a path on the hysteresis curve larger than the initial could be created which would lead to a growing exponential shape.

Another area of investigation is how temperature changes could affect the function of the circuit. The temperature would not only have an effect on the properties of the magnetic material in the inductor core but it could also potentially have an effect on the power supply used to provide an input to the MPC circuit.

The last suggested area of exploration would be an evaluation of the changes in the signature if the power supply or the load weren't modeled as perfectly consistent and never changing.

Appendix A – MATLAB Code to Create Nonlinear Inductor Mask

```
% Define base current and Flux for pu system
I_base = phi/L;
Phi_base = phi;

% Check first two points of the saturation characteristic
if ~all(all(sat(1:2,:) == [0 0; 1 1])), h=errordlg('The first two points
of the characteristic must be [0 0; 1 1]', 'Error');
    uiwait(h);
end

% Complete negative part of saturation characteristic
[npoints,ncol]=size(sat);
sat1=[sat ; -sat(2:npoints,:)];
sat1=sort(sat1);

% Current vector (A) and flux vector (V.s)
Current_vect=sat1(:,1)*I_base;
Flux_vect=sat1(:,2)*Phi_base;
```

Appendix B – MATLAB Code to Create Nonlinear Resistor Function

```
A=5.3/pi*1e-4;  
B=2.6;  
C=3;  
x=-6:0.11:6;  
y=A*atan((x/B));  
plot(x,y)
```

Appendix C – MATLAB Code to Calculate Pulse Delay

```
% Stephen Hartzell
% AFIT - RA
% 12-29-2011
% Last Revised: 12-29-2011
%% EXPLANATION
% This script requires a structure VoltageData output from simulink.
This script assumes there are three voltage signals saved in this
structure.
%% Declare new variables
t = VoltageData.time;
X1 = VoltageData.signals(1).values;
X2 = VoltageData.signals(2).values;
X3 = VoltageData.signals(3).values;

% Create logical array to find where the signal reaches and falls to 1%
of the maximum value
X1_truth = X1 > .01*max(X1);
if X1_truth(1)
    error('This method will not work if the signal starts in the on')
end
X2_truth = X2 > .01*max(X2);
X3_truth = X3 > .01*max(X3);

% Find points where each pulse of the signal starts and stops. Each
point is one less than it should be. This is why there is a plus 1 when
calculating X1_start and X1_end, etc.
dX1 = X1_truth(2:end) - X1_truth(1:end-1);
dX2 = X2_truth(2:end) - X2_truth(1:end-1);
dX3 = X3_truth(2:end) - X3_truth(1:end-1);

% Find the points at which the pulses start and stop
X1_start = find(dX1 == 1)+1;
X2_start = find(dX2 == 1)+1;
X3_start = find(dX3 == 1)+1;
X1_end = find(dX1 == -1)+1;
X2_end = find(dX2 == -1)+1;
X3_end = find(dX3 == -1)+1;
if length(X1_start) ~= length(X3_start)
    error('There must be as many input pulses as output pulses')
end

% Calculate the delay between the input and output
Delay = zeros(length(X1_start),1);
for ii = 1:length(X1_start)
    Delay(ii) = t(X3_start(ii)) - t(X1_start(ii));
end

figure(1)
stem(Delay)
clear X1_truth X2_truth X3_truth ii
```

Bibliography

- [1] Bailey, William. Class notes, PHYS 624, High Power Microwaves. School of Engineering and Management, Air Force Institute of Technology, Wright-Patterson AFB OH, Winter 2011.
- [2] Bluhm, Hansjoachim. *Pulsed Power Systems: Principles and Applications*, Berlin: Springer-Verlag, 2006.
- [3] Sampayan, Stephen. "Timing Instability in the Magnetically Switched Melville Line." Unpublished Report, Lawrence Livermore National Laboratory, Livermore, CA.
- [4] Roche, Stephan. "Solid State Pulsed Power Systems." Physique & industrie. http://www.purco.qc.ca/ftp/Steven%20Mark/mannix/solid_state_pulsed_power.pdf. 14 December 2011.
- [5] NDT Resource Center. "The Hysteresis Loop and Magnetic Properties." Excerpt from education resources. <http://www.ndt-ed.org/EducationResources/CommunityCollege/MagParticle/Physics/HysteresisLoop.htm>. 10 January 2012.
- [6] Dixon, Lloyd. "An Electrical Circuit Model for Magnetic Cores." Unitrode Corporation seminar. <http://www.ti.com/lit/ml/slup109/slup109.pdf>. 14 December 2011.
- [7] Choi, Jaegu. "Introduction of the Magnetic Pulse Compressor (MPS) - Fundamental Review and Practical Application," *Journal of Electrical Engineering & Technology*, 3: 484-492 (2010).
- [8] Sampayan, S.E., F.W. Chambers, F.J. Deadrick, W.A. Niven, C.W. Ollis, A.N. Payne, V.L. Renbarger, E.T. Scharlemann, W.C. Turner, and J.A. Watson. "Performance Characteristics of an Induction Linac Magnetic Pulse Compression Modulator at Multi-kilohertz Pulse Repetition Frequencies," *Proceedings of the IEEE 1991 Particle Accelerator Conference*, San Fransisco, CA, May 1991.
- [9] Chua, Leon and Keith Stromsmoe. "Lumped-Circuit Models for Nonlinear Inductors Exhibiting Hysteresis Loops," *IEEE Transaction on Circuit Theory*, 4: 564-574 (November 1970).
- [10] Melville, W.S. "The Use of Saturable Reactors as Discharge Devices for Pulse Generators," *Proceedings of the IEEE Radio and Communication*, 185-204 (1951).

REPORT DOCUMENTATION PAGE			<i>Form Approved</i> <i>OMB No. 074-0188</i>		
The public reporting burden for this collection of information is estimated to average 1 hour per response, including the time for reviewing instructions, searching existing data sources, gathering and maintaining the data needed, and completing and reviewing the collection of information. Send comments regarding this burden estimate or any other aspect of the collection of information, including suggestions for reducing this burden to Department of Defense, Washington Headquarters Services, Directorate for Information Operations and Reports (0704-0188), 1215 Jefferson Davis Highway, Suite 1204, Arlington, VA 22202-4302. Respondents should be aware that notwithstanding any other provision of law, no person shall be subject to any penalty for failing to comply with a collection of information if it does not display a currently valid OMB control number.					
PLEASE DO NOT RETURN YOUR FORM TO THE ABOVE ADDRESS.					
1. REPORT DATE (DD-MM-YYYY) 22 Mar 2012		2. REPORT TYPE Master's Thesis		3. DATES COVERED (From - To) Aug 2010 - Mar 2012	
4. TITLE AND SUBTITLE Timing Variations in a Magnetic Pulse Compression Circuit			5a. CONTRACT NUMBER		
			5b. GRANT NUMBER		
			5c. PROGRAM ELEMENT NUMBER		
6. AUTHOR(S) Oliver, Jeremy S., Capt, USAF			5d. PROJECT NUMBER N/A		
			5e. TASK NUMBER		
			5f. WORK UNIT NUMBER		
7. PERFORMING ORGANIZATION NAMES(S) AND ADDRESS(S) Air Force Institute of Technology Graduate School of Engineering and Management (AFIT/ENV) 2950 Hobson Way, Building 640 WPAFB OH 45433-8865			8. PERFORMING ORGANIZATION REPORT NUMBER AFIT/GE/ENG/12-31		
9. SPONSORING/MONITORING AGENCY NAME(S) AND ADDRESS(ES) National Air and Space Intelligence Center John Braun; William Berglund 4180 Watson Way WPAFB, OH 45433 257-2905, john.braun@wpafb.af.mil; 522-4826, william.berglund@wpafb.af.mil			10. SPONSOR/MONITOR'S ACRONYM(S) NASIC		
			11. SPONSOR/MONITOR'S REPORT NUMBER(S)		
12. DISTRIBUTION/AVAILABILITY STATEMENT APPROVED FOR PUBLIC RELEASE; DISTRIBUTION IS UNLIMITED					
13. SUPPLEMENTARY NOTES This material is declared a work of the U.S. Government and is not subject to copyright protection in the United States.					
14. ABSTRACT The magnetic pulse compression (MPC) circuit uses saturable core inductors and capacitors to compress the width of a pulse. This substantially increases the peak power of the initially applied pulse. The saturable inductor exhibits a hysteresis curve behavior. One particular problem with these MPC circuits is timing variances in the pulse rate of the system. This work models the unique characteristics and signatures of the timing variations of magnetic switches and pulse compressors. The hysteresis curve of the saturable inductor was created by using a nonlinear inductor and a nonlinear resistor in parallel as a substitute for saturable inductors. The circuit was built in MATLAB and simulations were run to determine the effectiveness of the pulse compression as well as the timing delays. A signature resembling a decaying exponential was then able to be recorded from the simulations. This shape was caused by the hysteresis curve not resetting to the initial state on the B-H plane after the first pulse is applied and it achieving a steady state at some smaller B-H curve after several pulses.					
15. SUBJECT TERMS magnetic switch; magnetic pulse compression; Melville line; saturable inductor					
16. SECURITY CLASSIFICATION OF:			17. LIMITATION OF ABSTRACT	18. NUMBER OF PAGES	19a. NAME OF RESPONSIBLE PERSON Andrew J. Terzuoli, PhD, ENG
a. REPORT	b. ABSTRACT	c. THIS PAGE			19b. TELEPHONE NUMBER (Include area code) (937) 255-3636, x 4717 (Andrew.terzuoli@afit.edu)
U	U	U	UU	66	